Figure S1, related to Figure 1. CP2 penetrates the blood brain barrier.

A

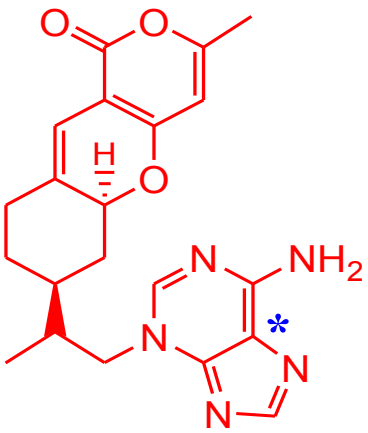

[C14]-CP2
Uniformly labeled adenine

B

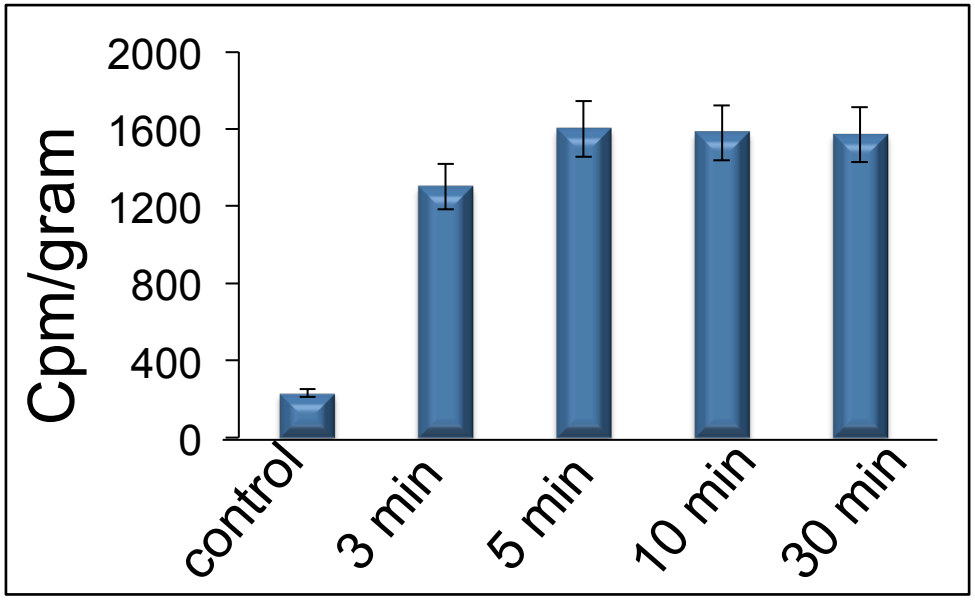

C

Time (min)	Average concentration of CP2 in plasma (mg/L)	
	IV route	po route
5	33.1 ± 12.2	
15	48.1 ± 3.4	5 ± 0.2
30	44.8 ± 2.1	5.3 ± 1.7
60	24.5 ± 5.9	10.7 ± 0.6
120	13.4 ± 1	7.3 ± 1.3
240	13.96 ± 0.7	5 ± 0.4
360	13.9 ± 0.5	3.4 ± 0.2
AUC (mg.min/L)	4856.8	2077.9
F	1	0.43

D

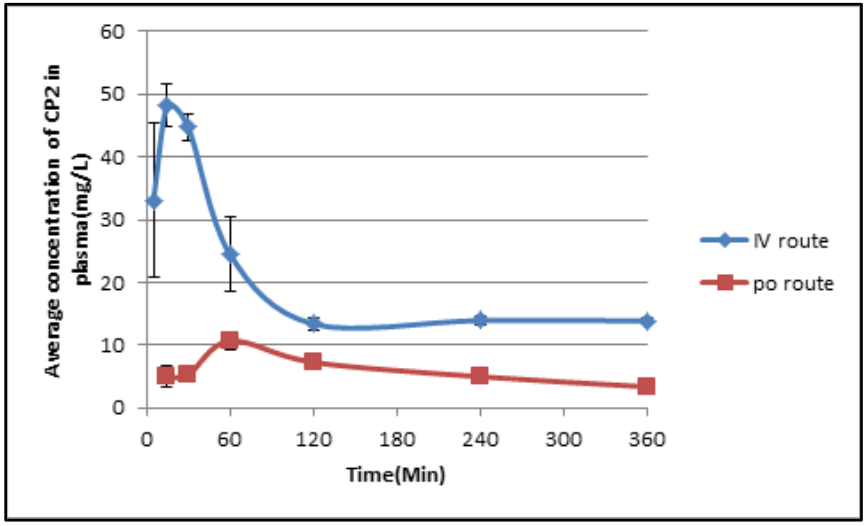

Figure S2, related to Figure 1. FAD mice treated with CP2 through life were well groomed and did not differ from NTG animals.

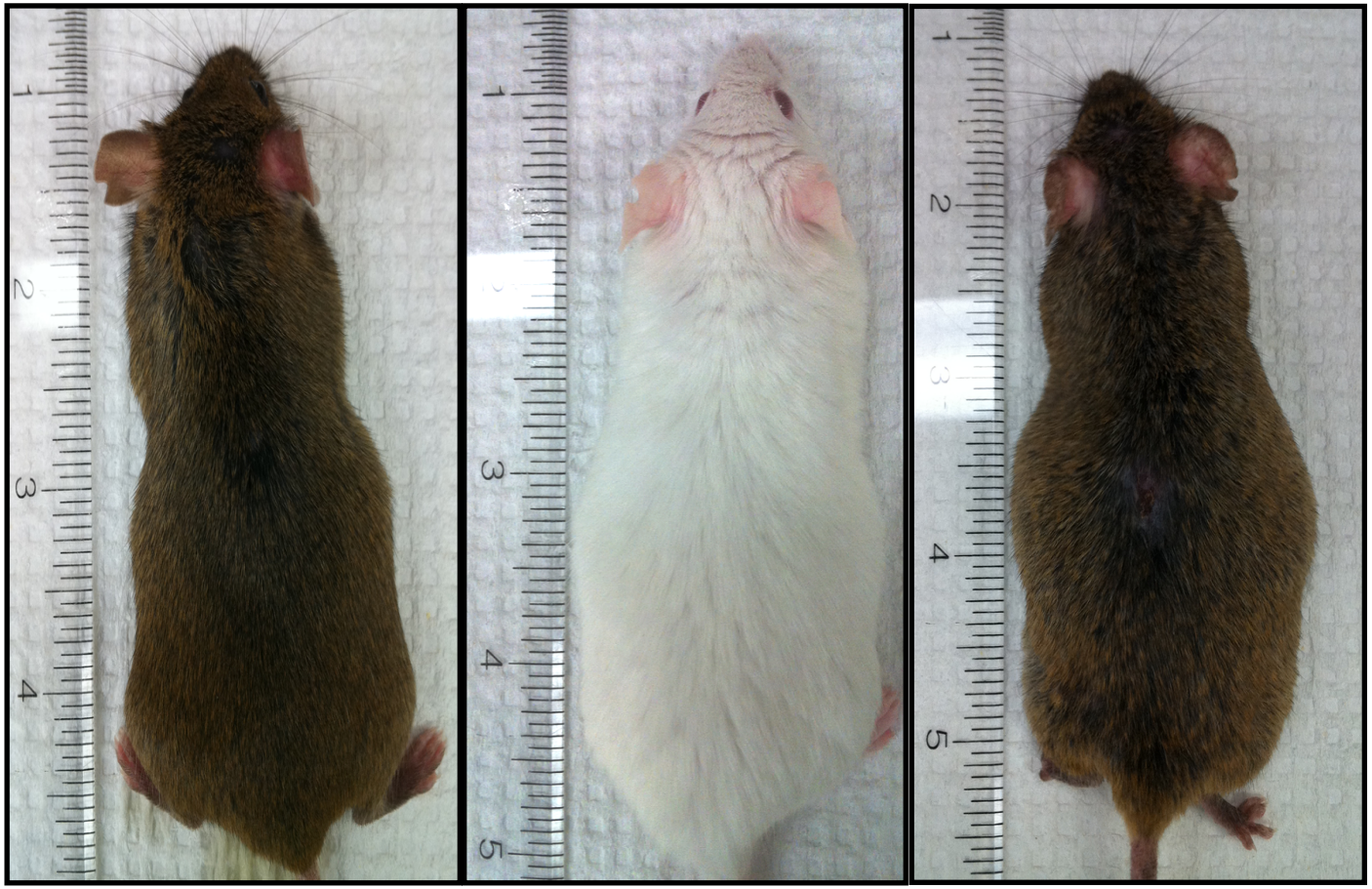

Figure S3, related to Figure 3. CP2 treatment reduces levels of amyloid plaques in the brain of FAD mice.

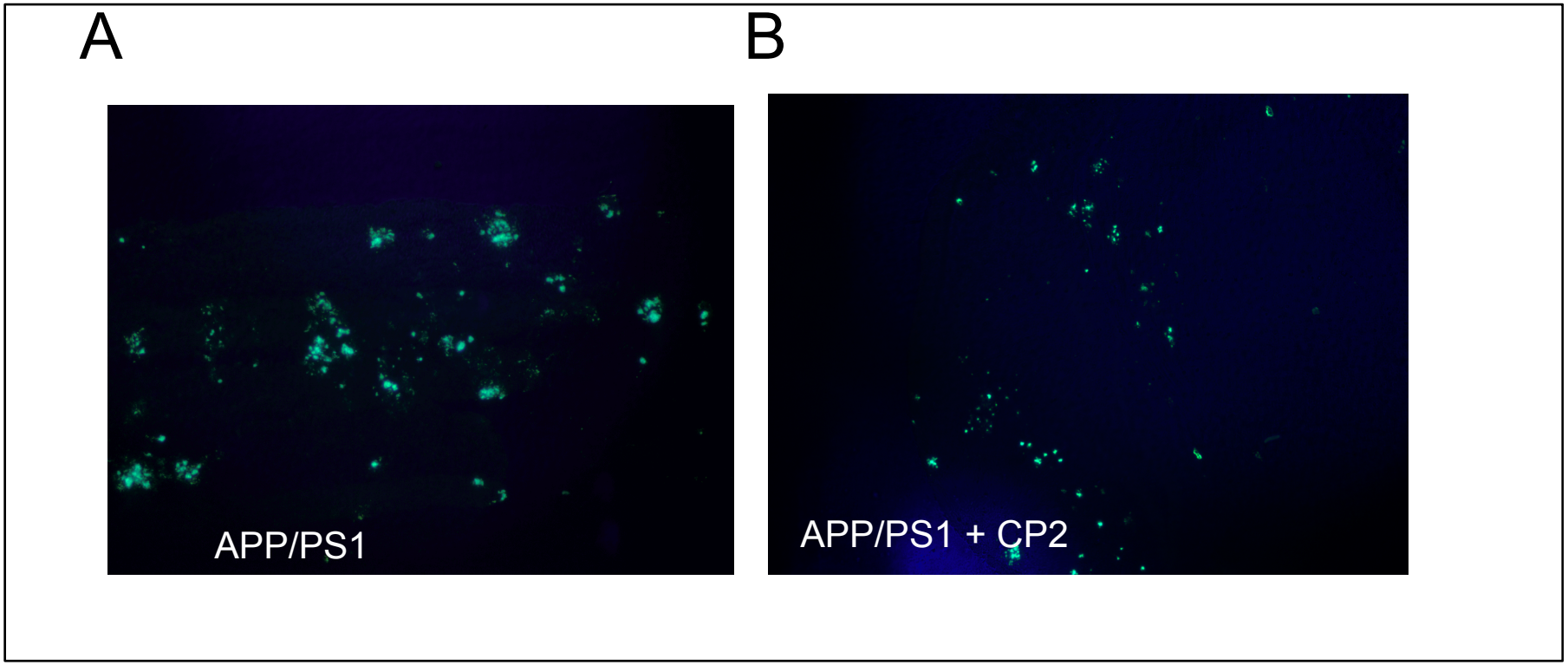

Figure S4, related to Figure 3. CP2 accumulates in heavy mitochondria fractions isolated from the brain of WT and APP/PS1 mice.

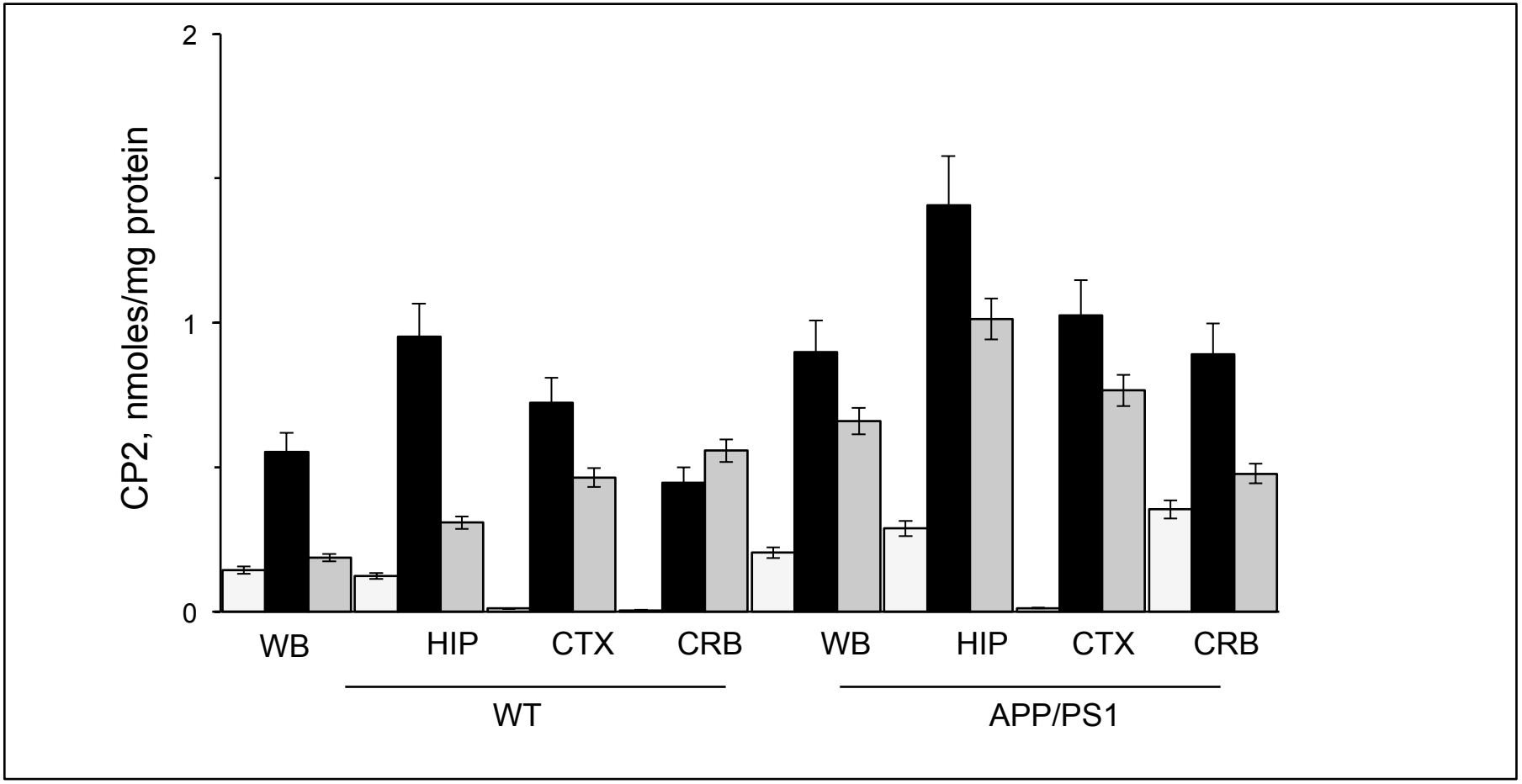

Figure S5, related to Figure 4. Mitochondrial energetics in primary neurons treated with CP2 measured using a Seahorse XF24 Extracellular Flux Analyser. and citrate synthase assay in brain tissue of CP2-treated WT and APP/PS1 mice

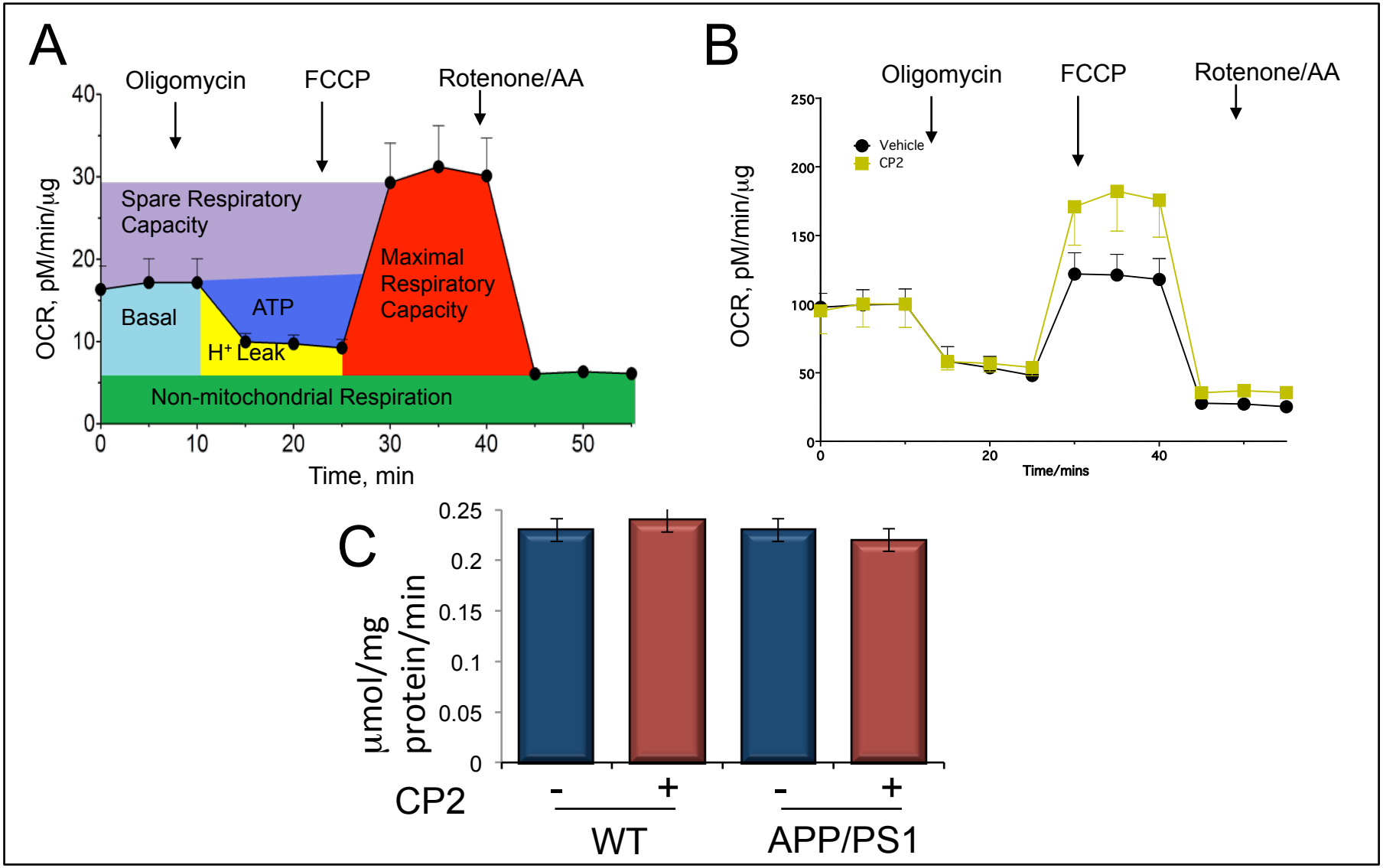

Figure S6, related to Figure 5. Gene expression profile in hippocampus of WT and APP/PS1 mice treated with CP2 for 4 months.

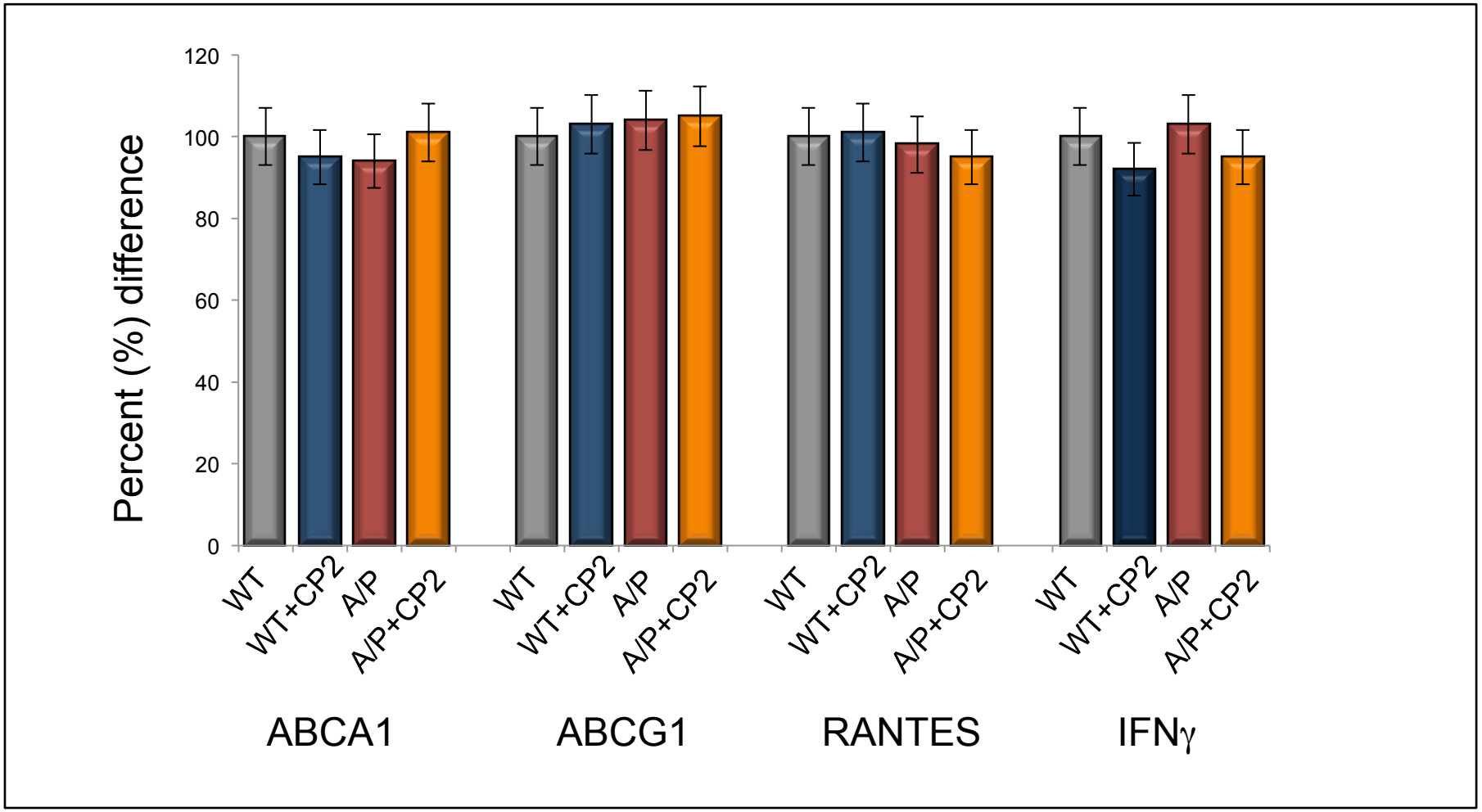

Figure S7, related to Figure 6. Quantification of western blots from Figure 6 using densitometry.

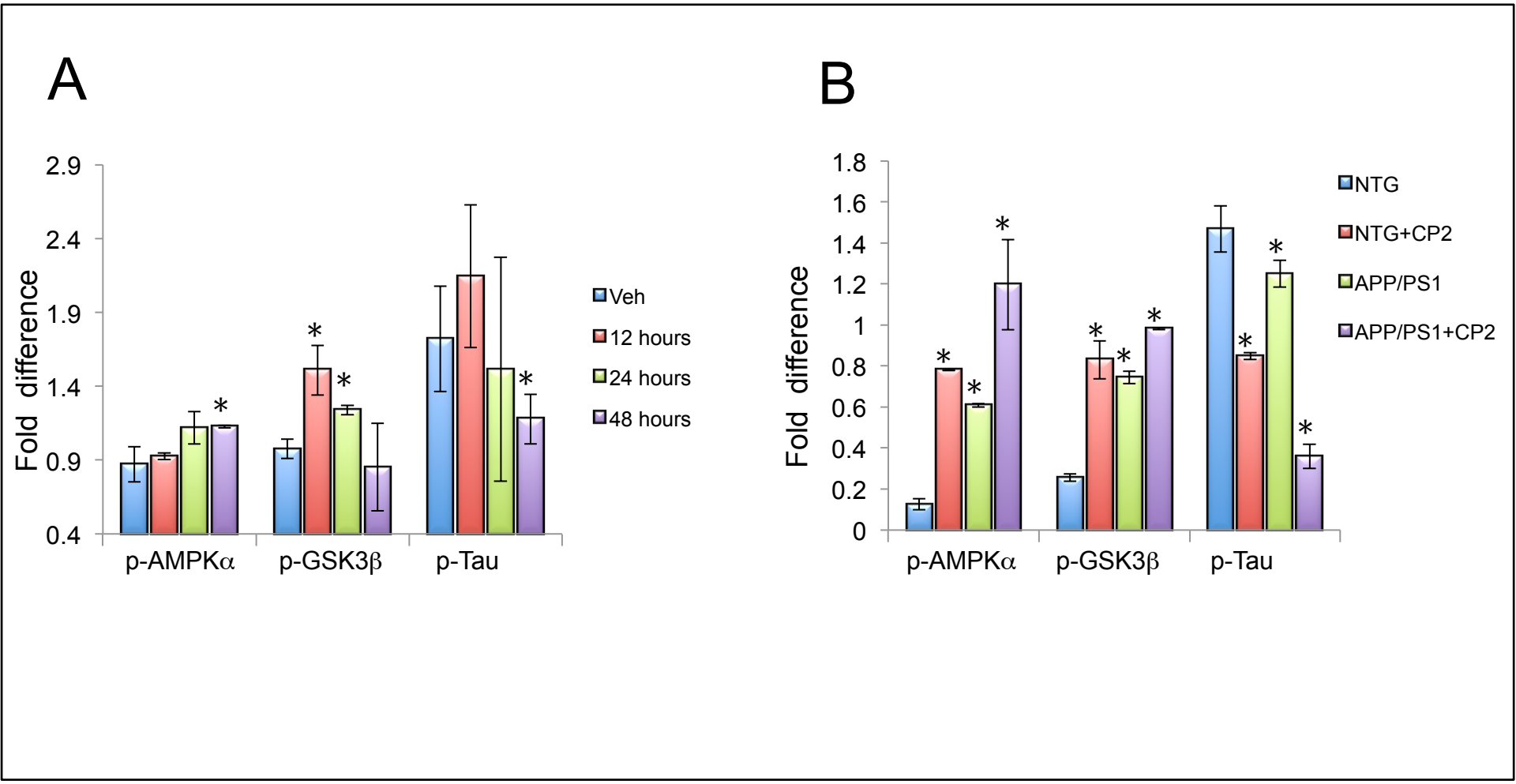

Supplemental Figure Legends

Figure S1, related to Figure 1. CP2 Penetrates the Blood Brain Barrier.

The study was undertaken to determine whether CP2 penetrates the BBB, and establish its bioavailability in the brain and plasma. (**A, B**) C14-labeled CP2 (**A**), 0.35 mCi/mg; 25 mg/kg, was injected into the abdomen of five C57BL/6 mice. Animals were anesthetized, perfused with saline, and brain was removed at indicated time points (**B**). The radioactivity in the brain was measured by liquid scintillation count and normalized by tissue weight. (**C,D**) Results of pharmacokinetics study of CP2 (25 mg/kg body weight) delivered to C57BL/6 male mice (n=3) via intravenous (IV) route and to female mice (n=3) orally (PO route). The maximal plasma concentration following PO route is 10.7 µg/ml, equivalent to 27.2 µM. The $t_{1/2}$ values following drug administration are around 58 min and 231 min for IV and PO, respectively. Areas under the curves (AUC) are 4856.8 and 2077.9 for IV and PO, respectively. The bioavailability (F) is estimated at 43%.

Figure S2, related to Figure 1. FAD Mice Treated With CP2 Through Life Did Not Differ From NTG Animals.

PS1 and APP mice treated with CP2 through life till 14 months of age were well groomed and did not differ by size or appearance from age and sex-matched NTG animals. 50 weeks old females are shown.

Figure S3, related to Figure 3. CP2 Treatment Reduces Levels of Amyloid Plaques In the Brain of FAD Mice.

(**A**) The example of the accumulation of amyloid plaques in the brain tissue of 7 months old APP/PS1 mouse visualized using immunofluorescence with biotinylated 4G8 antibody followed by incubation with Alexa Fluor 488-conjugated streptavidin. (**B**) Amyloid plaques in the brain

tissue of 7 months old APP/PS1 mouse were significantly (~50%) reduced after 4 months of CP2 treatment. Detection as in (**A**).

Figure S4, related to Figure 3. CP2 Accumulates in Enriched Mitochondria Fractions Isolated From the Brain of WT and APP/PS1 Mice.

Concentrations of CP2 measured using HPLC in the brain tissue of wild type (WT) and APP/PS1 mice (A/P) treated with 25 mg/kg/daily (*ad libitum* via drinking water) for 2 months. Mice were 5 months old at the time of tissue collection. WB – whole brain; HIP – hippocampus; CTX – cortex; CRB – cerebellum. White bar – crude nuclear, black bar – heavy mitochondria, and gray bar – cytosolic fractions.

Figure S5, related to Figure 4. Mitochondrial Primary Neurons Treated With CP2 Measured With a Seahorse XF24 Extracellular Flux Analyser, and Citrate Synthase Activity in Brain Tissue of CP2-treated WT and APP/PS1 Mice.

(**A**) Parameters of mitochondrial energetics measured using a Seahorse XF24 Extracellular Flux Analyser. OCR, oxygen consumption rate; AA – antimycin A. (**B**) OCR measurements in CP2- and vehicle-treated primary cortical neurons form WT mice normalized per basal oxygen consumption rate. Note similar decrease after the addition of oligomycin and the increase in spare respiratory capacity in CP2-treated neurons after the addition of FCCP. (**C**) Mitochondrial oxidative capacity measured in the brain tissue of WT (n = 5) and APP/PS1 mice (n = 5) treated with 25 mg/kg/day of CP2 for 4 months using citrate synthase assay.

Figure S6, related to Figure 5. **Gene Expression Profile in Hippocampus of WT and APP/PS1 Mice Treated With CP2 for 4 Months.**

Hippocampal brain tissue from NTG and APP/PS1 mice treated with 25 mg/kg/day of CP2 for 4 months was examined for gene expression of markers of inflammation (iNOS, RANTES and

interferon-gamma, IFNg), cholesterol efflux (ABCA1 and ABCG1) and house-keeping gene (beta-actin) using isolated RNA and qRT-PCR. The expression levels of each of the genes was normalized to the expression levels in untreated NTG mice, which was set as 100% after normalization for beta-actin levels. Experiment was conducted twice in independent cohorts of mice; 5 mice in each group were taken into analysis.

Figure S7, related to Figure 6. Quantification of Western Blots From Figure 6 Using Densitometry.

(A) Levels of p-AMPKα, p-GSK3β, and p-Tau in primary cortical neurons (P1) from APP/PS1 mice treated with CP2 (2 μM) over 48 hrs (**Figure 6)** normalized to tubulin levels. (**B)** Levels of p-AMPKα, p-GSK3β, and pTau in the brain tissue of NTG and APP/PS1 mice treated with CP2 (25 mg/kg/day, 2 months) compared to untreated animals (**Figure 6)** normalized to tubulin levels. *P < 0.05.

Supplemental Table 1, related to Figures 1 and 2.

CP2 concentration in the brain tissue of mice born from the CP2-treated parents and of adult mice treated with 25 mg/kg/daily (in drinking water *ad libitum*) over different periods of time.

Supplemental Table 2, related to Figures 1 and 2.

Levels of CP2 in various organs in wild-type mice treated with 25 mg/kg/daily (in drinking water *ad libitum*).

Supplemental Table 3, related to Figure 5.

Cluster analysis of multiple molecular dynamics simulations of CP2-bound FMN subunit of human complex I at 300 K and 1 atm.

SUPPLEMENTAL METHODS.

Chemicals

CP2 was prepared according to our published procedures (1) and purified using a preparative HPLC system, Jupiter C18, 10-μ column (Phenomenex, Torrance, CA, USA); running solvent system: H2O:CH3CN:CF3CO2H = 20:80:0.1, and identified by ^{1}H and ^{13}C NMR, IR, MS (matrix-assisted laser desorption ionization and electrospray ionization), and elemental analyses.

Animals

The following mice were used in the study: APP_{SWE} (K670N, M671L) (2); PS1 (M146L) (3); double transgenic APP/PS1 (4); non-transgenic (NTG) littermates; and C57BL/6 wild-type mice (WT). Genotypes were determined by PCR as described in (5). All animals were kept on a 12 h–12 h light-dark cycle, with a regular feeding and cage-cleaning schedule. Equal number of animals of both sexes was used in each study unless specified otherwise. Animals were randomly selected to study groups based on the age, sex and genotype. The number of animals in each group was determined based on the 95% of chance to detect changes in 30 - 50% of animals. The following exclusion criteria were established: significant (15%) weight loss, changing in the grooming habits (hair loss), pronounced motor dysfunction (paralyses), or other visible sings of distress (unhealed wounds).

Animal treatment

Life-long, chronic CP2 treatment

APP and PS1 breeders on standard diet were given 25 mg/kg/day of CP2 in drinking water *ad libitum*. Water consumption and animal weight was monitored to adjust CP2 concentrations (Figure 1). After weaning, F1 mice continued to receive CP2 (25

mg/kg/day) in drinking water through 14 months of age. F1 generation APP and PS1 mice were bred after reaching maturity at 2 months of age. The F2 P0-P1 pups were used for neuronal plating and axonal trafficking experiments. A battery of memory and behaviour tests was applied to P and F1 animals in the beginning and at the termination of the study. Organs were harvested and subjected to histopathological examination. CP2 measurements, EM, gene expression analysis, and western blot analysis.

CP2 treatment in pre-symptomatic APP/PS1 mice

WT and APP/PS1 mice were given CP2 (25 mg/kg/day) or vehicle-containing water (0.05% DMSO) starting at 2.5 months of age. Animals were housed individually, water consumption and weight was monitored weekly. Animals were subjected to behaviour and memory tests before treatment, and at 2 or 4 months after treatment. Animals were sacrificed 4 months after treatment; brain tissue was collected for experiments.

Behaviour tests were carried out in the light phase of circadian cycle with at least 24 h between each assessment. More than one paradigm ran within 1 week, however, no more than two separate tests were run on the same day. Tests were repeated at the same time of the day for 5 consecutive days. Investigators blinded to the animal genotypes and treatments conducted the analyses.

Locomotor activity

Spontaneous locomotor activity was measured in bright lit (500 lux) Plexiglas chambers (41cm × 41 cm) that automatically recorded activity via photo beam breaks (Med Associates, VT) as described in (6). The chambers were located in sound-attenuating cubicles and contained two sets of 16 pulse-modulated infrared photobeams to

automatically record X–Y ambulatory movements at a 100 ms resolution (Med Associates, Lafayette, IN). Data was collected continually over a single 10 min trial at 30 sec interval for 5 consecutive days.

Hanging bar

Balance and general motor function were assessed using the hanging bar test. Mice were lowered onto a parallel rod (D< 0.25 cm) placed 30 cm above a padded surface. Mice were allowed to grab the rod with their forelimbs, after which they were released and scored for their success (pass or failure) in holding onto the bar for 30 seconds. Mice were allowed three attempts to pass the bar test. Any one successful attempt to hold onto the bar was scored as a pass. The percentage of animals that fell (and failed the test) was measured with age and recorded as a percent of the total number of animals tested.

Stationary rotarod

For stationary rotarod, mice were allowed to stay on the rod rotating at 10 or 20 rpm for three attempts; the test time was 2 min. Time to fall was recorded for each mouse for all three attempts. Mice were tested for 5 consecutive days, at the same time of the day; the best time of three attempts was averaged over 5 days.

Accelerating rotarod

Mice were allowed to stay on the rotarod (Ugo Basile, Varese, Italy) that started rotation at 2 rpm and progressively accelerated to 50 rpm over a 5-min period. The latency of each animal to fall was recorded for three consecutive trials for 3 consecutive days. Latency across trials was analyzed.

Novel Object Recognition (NOR) Test

The onset of memory deficit was estimated using NOR test paradigm as described in (7). We used candles with various scents (apple or cherry). The number of interrogations of each object was manually assessed by an investigator blinded to the treatment groups. The number of interrogations of the novel object was divided by the number of investigations of the control object to generate a discrimination index. Intact recognition memory produces a discrimination index of 1 for the training session and a discrimination index greater than 1 for the test session, consistent with greater interrogation of the novel object.

T - maze

Each animal was acclimated in the center of a walled T-maze for 30 seconds before the guillotine doors were released. Animal was allowed to freely explore the maze for a single 5-min trial during which the sequence and total number of arm choices were recorded (8). Spontaneous alteration, expressed as a percent, was calculated according to the method of Arendash (9). If an animal made the following sequences of arm selections (A, B, C, B, A, C, A, B), the total alternation opportunities would be six (total entries minus two) and the percent of alteration would be 67% (four out of six).

Histopathological examination

NTG female animals treated with CP2 starting *in utero* for 6 months and untreated animals of the same age were sacrificed by cervical dislocation; brain, heart, lungs, liver, spleen and kidneys were removed, and placed in 10% formalin solution. Histopathological examination was conducted in Veterinary Diagnostic Laboratory (Manhattan, KS). All examined tissues from CP2-treated animals were similar to tissue of untreated mice.

CP2 bioavailability

Experiment #1. 0.35 mCi/mg; 25 mg/Kg of C14-labeled CP2 was injected into the abdomen of five C57BL/6 mice. Animals were anesthetized, perfused with saline, and brain was removed at 3, 5, 10 and 30 min post-injection. The radioactivity in the brain was determined by liquid scintillation count and normalized by tissue weight.

Experiment #2. We next established pharmacokinetics of CP2 (25 mg/kg body weight) delivered to C57BL/6 male mice (n=3) via intravenous (IV) route and to female mice (n=3) orally via gavage (PO route). The maximal plasma concentration of CP2 was measured using HPLC as described below. Plasma concentration of CP2 following PO route was 10.7 μg/ml, equivalent to 27.2 μM. The $t_{1/2}$ values following drug administration were around 58 min and 231 min for IV and PO, respectively. Areas under the curves (AUC) were 4856.8 and 2077.9 for IV and PO, respectively. The bioavailability (F) was estimated at 43%.

Quantification of CP2 in tissue

Animals were sacrificed by cervical dislocation. Organs from control and CP2-treated animals were harvested on ice and immediately flash frozen in liquid nitrogen. On the day of analysis, tissue was brought to room temperature, transferred to a Petri dish containing 1 ml of deionized water, and minced with razor blade. The mixture was diluted with 15 ml of water and transferred to a 50-ml conical vial. To the solution, 20 mg of sodium bicarbonate was added, stirred, followed by the addition of a solution of 20 ml of a 9:1 mixture of ethyl acetate and 1-propanol. The resulting mixture was sonicated for 40 minutes, transferred to a separatory funnel, and the organic layer was separated. The aqueous layer was extracted twice with 20 mL each of ethyl acetate and 1-propanol (9:1). The organic layers were combined and washed with 10 mL of brine, dried over

anhydrous $MgSO_4$, filtered and concentrated. The residue was dissolved in 0.4 mL of 1-propanol and filtered through a Fisher 0.2 μm filter. The original flask containing the extract and the filter were rinsed twice with 0.4 ml each of 1-propanol followed by 0.2 ml rinsing of the filter with 1-propanol. The total volume of the combined filtrate was 0.8 ml. Concentration of CP2 was estimated by mixing the extraction from above to a known concentration of 1,2,4,5-benzenetetracarboxylic acid (BTA) at 1:1 ratio. The BTA was used as an internal standard to quantify CP2 concentration from the extracts. The extract-BTA mixture was co-injected and separated using a reverse phase HPLC with mobile phase using a gradient mixture of water and acetonitrile (containing 0.1% TFA in both solvents). The peak of CP2 elutes at 35 minutes. The amount of CP2 was determined from the ratio of the areas of the peaks of CP2 to the peaks of BTA in the co-injection. Moreover, the peak that has the same retention time as that of CP2 from the injection of the tissue extract was collected, and its mass was determined using an Applied Biosystem API 2000 LC/MS/MS mass spectrometer. A mass of 394.2 corresponding to M+1 of PQ1 was found in the mass spectra, and the fragmentation pattern of this M+1 mass is identical to that of the authentic CP2.

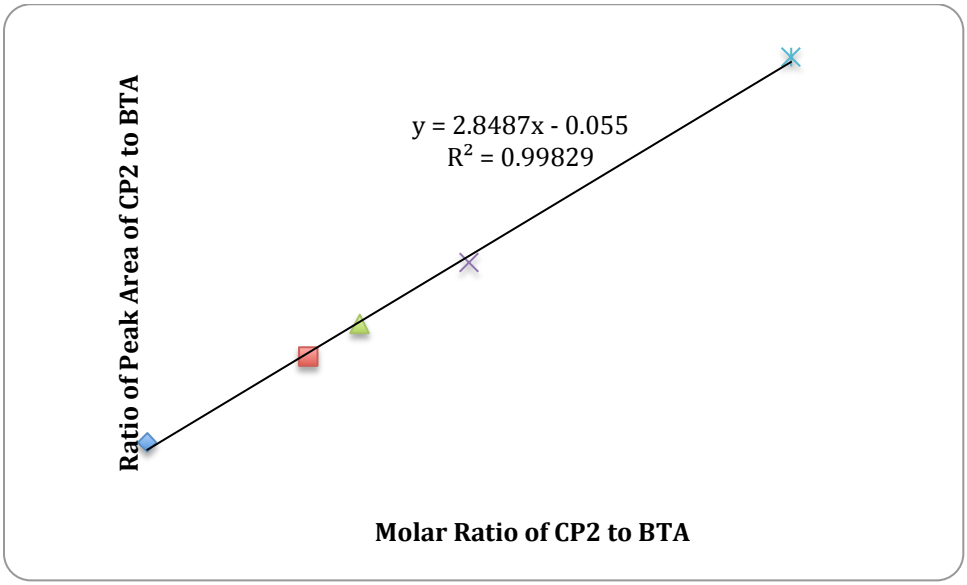

Graph 1. Correlation of different concentrations of CP2 and BTA using HPLC.

Levels of Soluble and Insoluble Aβ in Brain Tissue

Aβ plaques were visualized using confocal immunofluorescence and confocal microscopy as we described previously (10). Three brain slices were imaged per mouse. The average particle size of the plaques was determined using Image J 1.45 (rsbweb.nih.gov/ij/). The original colored image was converted to grey-scale (8-bit) image. The upper and lower threshold limits were adjusted so that the particles of interest could be analyzed correctly. Finally, the average size of the particles was obtained by selecting the "analyze particle" from the Image J window. The area of the particles to be analyzed was set from 10 pixel units to infinity in all cases. For each image the average particle size was obtained three times and the value was averaged.

Soluble Aβ levels were determined in brain tissue isolated from untreated (n=9) and CP2-treated (n=9) APP/PS1 mice 7 months old treated for 5 months. Brain tissue was sequentially homogenized in Tris-buffered saline (TBS), TBS buffer containing 1% Triton X-100 (TBS-TX), and 5 M guanidine in 50 mM Tris-HCl, pH 8.0 (Youmans et al., 2011). The levels of human Aβ40 and Aβ42 were determined by ELISA as previously described (Shinohara et al., 2013) using antibodies produced in-house as previously published (Kanekiyo, 2013).

Subcellular Localization of CP2 in Neurons

Primary cortical neurons from wild type mice were plated at 6 x 10^6 cells per 10-cm plate. After culturing for 7 days, cells were treated with 2 μM CP2 or vehicle (0.01% DMSO) for 24 h. Prior to procedure, neurons were washed with ice-cold PBS and resuspended in 0.5 ml of mitochondrial isolation buffer (MIBA) containing 10 mM Tris-

HCl, pH 7.4, 1 mM EDTA, 0.2 M D-mannitol, 0.05 M sucrose, 0.5 mM sodium orthovanadate, 1 mM sodium fluoride and 1× complete protease inhibitors (11). Cells were homogenized and lysed with the aid of a Teflon pestle. The crude nuclei (CN) fraction was isolated from the lysate by centrifugation at 500× *g* at 4 °C for 5 min. The remaining supernatant was centrifuged at 8000× g for 10 min at 4 °C, yielding the heavy mitochondrial (HM) and the cytoplasmic (CYTO) fractions. The HM pellet was washed twice with ice-cold MIBA prior to final suspension in 0.5 ml of MIBA buffer. Extraction and quantification of CP2 in CN, HM and CYTO fractions was done as described above. The integrity of mitochondria in enriched subcellular fractions was examined using electron microscopy. The purity of each enriched fraction was determined using western blot analysis with 20 *μ*g of protein and SDS-PAGE. After transfer to PVDF, immunoblot analysis was performed using the following antibodies: p62 nucleoporin (BD Transduction Laboratories, Lexington, KY); TOM 20 (Santa Cruz Biotechnology, Santa Cruz, CA); and Tau46 (Cell Signaling Technology, Danvers, MA).

Estimation of ATP levels

ATP levels in primary cortical neurons and mouse brain tissue were estimated using HPLC. Cells cultured for 6 days in 60 mm dishes were washed with PBS before addition of 0.25 ml perchloric acid (0.6 M with 1 mM EDTA). Acid-insoluble material was removed by centrifugation at 10,000 x g for 10 min and used for protein assay. Perchloric acid was neutralized with 2 M $KHCO_3$. Nucleotides were separated on a reversed-phase Discovery C18 columns (SIGMA, St. Louis, MO) with Hewlett-Packard series 1100 HPLC system (Agilent, Santa Clara, CA). Mobile phase A consisted of 100 mm potassium phosphate and 10 Mm tetrabutyl ammonium hydrogen sulphate (TBHS) dissolved in deionized water and adjusted to pH = 6.5 with potassium hydroxide, while

mobile phase B consisted of mobile phase A and methanol (40:60 v/v). HPLC separation was achieved using continuous gradient elution. The elution program was as follows: 0 min 100% A, 0% B; 5 min 50% A, 50% B; 10 min 50% A, 50% B; 18 min 100% A, 0% B. Finally, the program took a further 10 min to return to the initial conditions and stabilize. Flow rate of the mobile phase was 0.7 mL/min, while the injection volume was 200 µL. The total retention time was about 14 min and the gradient was run for 18 min to ensure full separation. Levels in brain tissue of WT and APP/PS1 mice treated with CP2 were estimated in the similar way. Levels of ATP and AMP in the samples were identified by comparison with retention time of standards, while the concentrations of ATP and AMP were determined using the external standard method. Protein concentration was determined using Bio-Rad reagent. ATP levels were expressed as nanomoles of ATP per microgram of protein. AMP/ATP ratio was calculated after normalization. Data were expressed as means from 6 individual sample replicates.

Neuronal cultures

Primary hippocampal and cortical neurons were cultured as described in (5, 12). Briefly, female pregnant mice were anesthetized with isoflurane on gestational day 17-18, and fetuses were rapidly removed. Fetal brains were extracted and placed in sterile HEPES-buffered saline (HBS) (pH 7.3). The cortices were dissected from each embryo and combined. Tissue was placed in 1 mg/mL papain (Warthington, NJ) in HBS for 20 min at 37°C. After two washes in HBS, the dissociated tissue was triturated in Dulbecco's modified Eagle's medium (DMEM) containing 10% Ham's F12 with glutamine (Gibco/BRL, Grand Island, NY), 10% heat inactivated fetal calf serum (Hyclone Laboratories Logan, UT) and 1x pen/strep antibiotic mixture. Cells were counted, diluted to $3.5x10^5$ cells/mL, and 2 mL of this stock was placed in each well of a 6-well dish

containing glass coverslips coated with poly-L-ornithine (1 mg/2 mL sterile borate buffer, pH 8.4). Plated cells were maintained in an incubator with 5% CO_2 at 37°C. After 72 h in culture, serum-containing medium was replaced with a serum-free Neurobasal-based medium (without glutamine, Gibco/BRL, Grand Island, NY) containing 1 x pen/strep antibiotic mixture and 1 x B27 supplement (Gibco/BRL, Grand Island, NY). Quantification of neurons and glial cells using specific antibody staining (GFAP for astrocytes, AB5804, Millipore, and neuron specific βIII-tubulin, ab18207, Abcam) demonstrates that neurons represent 95% of cultured cells. In cases where experiments required especially pure neuronal cultures, cells were treated with cytosine β-D-arabinofuranoside (Ara-C, Sigma, MO) to a final concentration of 2 μM after 3 and 5 days in culture to suppress proliferation of the glial cells. Such conditions resulted in obtaining fully developed pure cortical neurons exhibiting synaptic activity as judged by staining with synapsin antibody (ab8, Abcam). Neurons from neonatal mice (P1) were isolated from individual pups; genotyping was done prior to the day of experiment. All experiments were performed in neurons cultured for 7 days (DIC) unless specifically stated.

Mitochondrial Respiration

Mitochondrial respiration was determined in intact cortical neurons (E17) from WT mice using an XF24 Extracellular Flux Analyzer (Seahorse Biosciences, North Billerica, MA) as described in (13). Neurons were seeded in the 24 well plates at 1×10^4 cells per well and cultured for 6 – 7 days in Neurobasal media (5). Cells were treated with 2 μM CP2 or vehicle for 24 h before cells were placed in fresh bicarbonate-free DMEM containing 25 mM glucose and 0.2 mM pyruvate. Baseline OCR was assessed using 3 measurement loops consisting of a 3 min mix cycle, a 2 min delay cycle and a 3 min measurement cycle. Respiratory chain inhibitors were sequentially injected into the

wells, and ATP-coupled oxygen consumption was calculated as the fraction of the basal OCR sensitive to 0.75 *μ*M oligomycin, an ATP synthase inhibitor. The maximal uncoupled respiration rate was determined by depolarizing the mitochondrial membrane potential with 0.75 *μ*M FCCP (carbonylcyanide-4-(trifluoromethoxy)- phenylhydrazone), and non-mitochondrial respiration was determined as the activity remaining after inhibition of complexes I and III with 0.75 *μ*M rotenone and 0.75 *μ*M antimycin A, respectively. At the end of the experiments, cells were harvested and values were normalized to protein content of each well. Maximum respiratory capacity, spare respiratory capacity and respiratory state apparent ($State_{app}$) were determined as described in (14, 15).

Effect of CP2 on activity of mitochondrial complexes I–V

Experiments were done as described in (16)**.** Each assay was performed using enriched mitochondria fraction isolated from mouse brain homogenate subjected to three freeze–thaw cycles in liquid N_2 to expose enzymes. Isolated mitochondria were incubated on ice with different concentrations of CP2 for 1 min before addition of complex-specific assay substrates.

C**omplex I (**NA**DH:ubiquinone oxidoreductase)**

Activity of complex I in the presence of different concentration of CP2 (1 nM – 50 uM) was determined by measuring the absorbance at 340 nm caused by the oxidation of NADH. Rotenone was used as positive control.

C**omplex II (succinate dehydrogenase)**

Activity of complex II was measured by following the decrease in absorbance at 600 nm caused by the reduction of dichlorophenol indophenols. The specificity of the reaction was determined using specific complex II inhibitor atpenine A5.

C**omplex III (decylubiquinol cytochrome *c* oxidoreductase)**

Activity of complex III was measured by following the increase in absorbance at 550 nm caused by the reduction of cytochrome c. Antimycin A was used to avoid underestimation of antimycin A-resistant activity.

C**omplex IV (cytochrome *c* oxidase)**

Complex IV activity was measured by following the decrease in absorbance at 550 nm caused by the oxidation of reduced cytochrome c. The specificity of this reaction was determined using potassium cyanide.

Complex V (F1-ATPase)

The assay relies on linking the ATPase activity to NADH oxidation via the conversion of phosphoenolpyruvate (PEP) to pyruvate by pyruvate kinase (PK), and then pyruvate to lactate by lactate dehydrogenase (LDH) over 5 minutes at 340 nm. To determine the nonspecific activity, a 2 mmol/L solution of oligomycin was added before the mitochondria protein.

Axonal Trafficking Assay

Primary cortical neurons (P1) from individual neonatal mice born from CP2-treated APP and PS1 parents (**Figure 1**B) were plated and cultured for 7 days. Tissue was collected for genotyping. Analysis of axonal trafficking was performed using time-lapse imaging as described previously (5, 17). Briefly, mitochondria were visualized with tetramethylrhodamine, methyl ester (TMRM) (Molecular Probes, Eugene, OR) (final concentration 50 nM, 15 min incubation). TMRM were washed away with fresh F-12K (phenol red-free) medium prior to imaging. The experiments were performed using confocal microscope LSM 510 (Carl Zeiss Inc, Germany) with a Plan-Apochromat 100x (1.4 na) oil objective. Cells were incubated at 37°C during the time of recording. All recordings were started five minutes after the coverslip was placed on the microscopic

stage to allow equilibration of the sample. Laser was set up to 543 nm for excitation; emission was collected at 585 nm and greater. Axons were selected based on the lack of branching through the whole length. A total of 600 images were recorded per cell. Images were taken every 1 sec at highest scan speed (0.9 sec) for 10 min. Three different cells were imaged from one coverslip. Movies were analyzed using LSM 510 software that allowed animation of 600 images into a "movie". For analysis of axonal trafficking, each mitochondrion was traced from the first frame of the movie to the last. We recorded time and distance that particular organelle traveled in axons, and calculated velocities in anterograde (from the cell body) and retrograde (to the cell body) directions. Neurons (n = 22 - 27) from 3-5 independent platings with 200 - 300 individual mitochondria were taken into analysis for each genotype.

Theoretical model of the CP2-bound FMN subunit of human mitochondrial complex I

The homology model of FMN subunit of human mitochondrial complex I was generated by the Swiss-Model program (18) using the FMN subunit sequence from NCBI (Accession ID: P49821.4) and the crystal structure of bovine mitochondrial supercomplex I1III2IV1 (Protein Data Bank ID: 2YBB) as a template. The protonated CP2 in an extended conformation was optimized with the HF/6-31G*//HF/6-31G* method using the Gaussian 98 program (revision A.7; Gaussian, Inc.). CP2 was manually docked into the FMN binding site of the FMN subunit. This docking placed (*i*) the pyrone ring parallel to Tyr1104 to form off-center pi-pi interaction, (*ii*) the adeninium ring between Ala91 and Glu209 with the adeninium NH2 forming a hydrogen bond with the carboxylate of Glu174, and (*iii*) the methylenecyclohexane ring atop Gly207. The Fe_4S_4 cluster was then manually docked into the FMN subunit with the four iron cations in coordination with Cys379, Cys382, Cys385, and Cys425 according to the Fe_4S_4

coordination in the 2YBB crystal structure. The RESP charge of CP2 were generated by a published procedure (19, 20). The bond and angle parameters of Fe_4S_4 were generated according to the crystal structures of Fe_4S_4 complexes (21). The atomic charges of the Fe_4S_4 cluster were developed to make the total charge of the cysteinate-coordinated Fe_4S_4 cluster in the FMN subunit identical to the total charge of the oxidized ferredoxin ($[Fe_4S_4(SR)_4]^{2-}$) (22). The van der Waals parameters of the iron cation were taken from

http://personalpages.manchester.ac.uk/staff/Richard.Bryce/amber/cof/frcmod.hemall.

Topology and coordinate files were generated by the tLeAP module of AmberTools 13 (University of California, San Francisco). The resulting CP2 complex model was energy minimized by using SANDER of AMBER 11 (University of California, San Francisco) with AMBER forcefield FF12MC, dielectric constant of 1.0, and 100 cycles of steepest-descent minimization followed by 900 cycles of conjugate-gradient minimization. Developed by Y.-P.P., FF12MC is based on AMBER forcefield FF99 with changes of (*i*) reducing all atomic masses by tenfold (23), (*ii*) shortening C–H bond lengths by 10–14% (1.09 Å to 0.98 Å for the aliphatic; 1.08 Å to 0.93 Å for the aromatic) (24), and (*iii*) zeroing torsion potentials involving a nonperipheral sp^3 atom with reduction of the 1–4 interaction scaling factors of protein backbone torsions ϕ and ψ (from 2.00 to 1.00 for the van der Waals interaction; from 1.20 to 1.18 for the electrostatic interaction) (25). The energy-minimized complex was then solvated with 12,264 TIP3P water molecules (26) and energy-minimized for 100 cycles as above followed by 900 cycles of conjugate-gradient minimization to remove close van der Waals contacts using FF12MC. The resulting system was then heated from 0 to 300 K at a rate of 10 K/ps under constant temperature and volume, and finally simulated in 20 unique and independent all-atom, isothermal–isobaric, 50-ns, and low-mass molecular dynamics simulations using PMEMD of AMBER 11 with a periodic boundary condition at 300 K and 1 atm with

isotropic molecule-based scaling. All simulations used (*i*) a dielectric constant of 1.0, (*ii*) the Berendsen coupling algorithm (27), (*iii*) the Particle Mesh Ewald method to calculate long-range electrostatic interactions (28), (*iv*) a time step of 1.0 fs, (*v*) SHAKE-bond-length constraints applied to all the bonds involving the H atom, (*vi*) a protocol to save the image closest to the middle of the "primary box" to the restart and trajectory files, (*vii*) a formatted restart file, (*viii*) the recently reported alkali and halide ions parameters (29), (*ix*) a nonbonded cutoff of 8.0 Å, (*x*) default values of all other inputs of the PMEMD module. Trajectories were saved at 100-ps intervals in all simulations performed on 20 dedicated 12-core Apple Mac Pros with Intel Westmere (2.93 GHz). Cluster analysis using the PTRAJ module of AmberTools 13 with the average-linkage algorithm (30) (epsilon = 2.5 Å; RMS on :87-95@C*, :116-120@C*, :127@C*, :204@C*, :244-247@C*, :323@C*, :373-374@C*,:454@C*). This analysis identified 5 most populated clusters of the CP2 complex. The CP2 binding mode from the most populated cluster is shown in Figure 5E and F (Table S3).

Western blot analysis

Protein expression were determined in brain tissue and neurons as described in (5) using the following antibodies: p-AMPK (1:1000, Cell Signaling Technology, Danvers), AMPK (1:1000, Cell Signaling Technology, Danvers), p-GSK3β (1:1000, Cell Signaling Technology, Danvers), GSK3β (1:1000, Cell Signaling Technology, Danvers), pTau (1:1000, Cell Signaling Technology, Danvers), Tau (1:1000, Cell Signaling Technology, Danvers), Tubulin (1:5000, Sigma, St-Louis, MO), Synaptophysin (1:200, Santa Cruz Biotechnology, Santa Cruz, CA), Synapsin-1 (Cell Signaling Technology, 1 μg/μl), BDNF (1:200, Santa Cruz Biotechnology, Santa Cruz, CA), Tom 20 (1:200, Santa Cruz Biotechnology, Santa Cruz, CA); nucleoporin (1:1000, BD Biosciences, CA), donkey

anti-rabbit IgG conjugated with Horseradish Peroxidase (1:10000 dilution, GE Healthcare UK Limited, UK) and sheep anti-mouse IgG conjugated with Horseradish Peroxidase (1:10000 dilution, GE Healthcare UK Limited, UK) The following secondary antibodies were used: ZyMaxTM Goat Anti-Rabbit IgG (H**+**L) CyTM 5 conjugate and/or Alexa Fluor 488 goat anti-mouse IgG (H**+**L), Invitrogen; and analyzed using a PharosFX Plus Molecular Imager (Bio-Rad).

Supplemental references

1. Hua DH, Huang X, Tamura M, Chen Y, Woltkamp M, Jin L, Perchellet EM, Perchellet J, Chiang PK, Namatame I, et al. Syntheses and bioactivities of tricyclic pyrones. *Tetrahedron.* 200359):4795–803.
2. Hsiao K, Chapman P, Nilsen S, Eckman C, Harigaya Y, Younkin S, Yang F, and Cole G. Correlative memory deficits, Abeta elevation, and amyloid plaques in transgenic mice. *Science.* 1996;274(5284):99-102.
3. Duff K, Eckman C, Zehr C, Yu X, Prada CM, Perez-tur J, Hutton M, Buee L, Harigaya Y, Yager D, et al. Increased amyloid-beta42(43) in brains of mice expressing mutant presenilin 1. *Nature.* 1996;383(6602):710-3.
4. Holcomb L, Gordon MN, McGowan E, Yu X, Benkovic S, Jantzen P, Wright K, Saad I, Mueller R, Morgan D, et al. Accelerated Alzheimer-type phenotype in transgenic mice carrying both mutant amyloid precursor protein and presenilin 1 transgenes. *Nat Med.* 1998;4(1):97-100.
5. Trushina E, Nemutlu E, Zhang S, Christensen T, Camp J, Mesa J, Siddiqui A, Tamura Y, Sesaki H, Wengenack TM, et al. Defects in Mitochondrial Dynamics and Metabolomic Signatures of Evolving Energetic Stress in Mouse Models of Familial Alzheimer's Disease. *PLoS One.* 2012;7(2).

6. Lee MR, Hinton DJ, Song JY, Lee KW, Choo C, Johng H, Unal SS, Richelson E, and Choi D-S. Neurotensin receptor type 1 regulates ethanol intoxication and consumption in mice. *Pharmacology Biochemistry and Behavior.* 2010;95(2):235-41.

7. Buenz EJ, Sauer BM, Lafrance-Corey RG, Deb C, Denic A, German CL, and Howe CL. Apoptosis of hippocampal pyramidal neurons is virus independent in a mouse model of acute neurovirulent picornavirus infection. *Am J Pathol.* 2009;175(2):668-84.

8. Deacon RMJ, Nicholas J, and Rawlins P. T-maze alternation in the rodent. *Nature Protocols.* 2006;1(1):7-12.

9. Arendash GW, Gordon MN, Diamond DM, Austin LA, Hatcher JM, Jantzen P, DiCarlo G, Wilcock D, and Morgan D. Behavioral assessment of Alzheimer's transgenic mice following long-term Abeta vaccination: task specificity and correlations between Abeta deposition and spatial memory. *DNA Cell Biol.* 2001;20(11):737-44.

10. Maezawa I, Jin LW, Woltjer RL, Maeda N, Martin GM, Montine TJ, and Montine KS. Apolipoprotein E isoforms and apolipoprotein AI protect from amyloid precursor protein carboxy terminal fragment-associated cytotoxicity. *Journal of neurochemistry.* 2004;91(6):1312-21.

11. Okado-Matsumoto A, and Fridovich I. Subcellular distribution of superoxide dismutases (SOD) in rat liver: Cu,Zn-SOD in mitochondria. *The Journal of biological chemistry.* 2001;276(42):38388-93.

12. Trushina E, Heldebrant MP, Perez-Terzic CM, Bortolon R, Kovtun IV, Badger JD, 2nd, Terzic A, Estevez A, Windebank AJ, Dyer RB, et al. Microtubule destabilization and nuclear entry are sequential steps leading to toxicity in Huntington's disease. *Proc Natl Acad Sci U S A.* 2003;100(21):12171-6.

13. Wu M, Neilson A, Swift AL, Moran R, Tamagnine J, Parslow D, Armistead S, Lemire K, Orrell J, Teich J, et al. Multiparameter metabolic analysis reveals a close link between attenuated mitochondrial bioenergetic function and enhanced glycolysis dependency in human tumor cells. *Am J Physiol Cell Physiol.* 2007;292(1):C125-36.

14. Brand MD, and Nicholls DG. Assessing mitochondrial dysfunction in cells. *The Biochemical journal.* 2011;435(2):297-312.

15. Sansbury BE, Jones SP, Riggs DW, Darley-Usmar VM, and Hill BG. Bioenergetic function in cardiovascular cells: the importance of the reserve capacity and its biological regulation. *Chemico-biological interactions.* 2011;191(1-3):288-95.

16. Spinazzi M, Casarin A, Pertegato V, Salviati L, and Angelini C. Assessment of mitochondrial respiratory chain enzymatic activities on tissues and cultured cells. *Nature protocols.* 2012;7(6):1235-46.

17. Trushina E, Dyer RB, Badger JD, 2nd, Ure D, Eide L, Tran DD, Vrieze BT, Legendre-Guillemin V, McPherson PS, Mandavilli BS, et al. Mutant huntingtin impairs axonal trafficking in mammalian neurons in vivo and in vitro. *Mol Cell Biol.* 2004;24(18):8195-209.

18. Kiefer F, Arnold K, Kunzli M, Bordoli L, and Schwede T. The SWISS-MODEL Repository and associated resources. *Nucleic Acids Res.* 2009;37(Database issue):D387-92.

19. Cornell W.D., Cieplak P., Bayly C. I., Gould I. R., Merz K. M., Ferguson D. M., C. SD, Fox T., Caldwell J. W., and A. KP. A Second Generation Force Field for the Simulation of Proteins, Nucleic Acids, and Organic Molecules. *J Am Chem Soc.* 1995;117(5179-97.

20. Cieplak P, Cornell WD, Bayly C, and Kollman PA. Application of the multimolecule and multiconformational RESP methodology to biopolymers:

Charge derivation for DNA, RNA, and proteins. *J Comput Chem* 1995;16(1357 - 77.

21. Hagen KS, Watson AD, and Holm RH. Analogs of the [Fe4s4]+ sites of reduced ferredoxins - single-step synthesis of the clusters [Fe4s4(Sr)4]3- and examples of compressed tetragonal core structures. *Inorganic Chemistry* 1984;23(2984-90.
22. Greenwood NN, and Earnshaw A. *Chemistry of the elements.* 1997.
23. Pang Y-P. Low-mass molecular dynamics simulation: A simple and generic technique to enhance configurational sampling. *Biochem Biophys Res Commun.* 2014;452(3):588–92.
24. Pang Y-P. At least 10% shorter C–H bonds in cryogenic protein crystal structures than in current AMBER forcefields. *Biochem Biophys Res Commun.* 2015;458(2):352–5.
25. Pang Y-P. Use of 1–4 interaction scaling factors to control the conformational equilibrium between α-helix and β-strand. *Biochem Biophys Res Commun.* 2015;457(2):183–6.
26. Jorgensen WL, Chandreskhar J, Madura JD, Impey RW, and Klein ML. Comparison of simple potential functions for simulating liquid water. *J Chem Phys* 1983;79(926-35.
27. Berendsen HJC, Postma JPM, van Gunsteren WF, Di Nola A, and Haak JR. Molecular dynamics with coupling to an external bath. *J Chem Phys.* 1984;81(3684–90.
28. Darden TA, York DM, and Pedersen LG. Particle mesh Ewald: An N log(N) method for Ewald sums in large systems. *J Chem Phys.* 1993;98(10089–92.
29. Joung IS, and Cheatham TE. Determination of alkali and halide monovalent ion parameters for use in explicitly solvated biomolecular simulations. *J Phys Chem B* 2008;112(9020-41.

30. Shao J, Tanner SW, Thompson N, and Cheatham III TE. Clustering molecular dynamics trajectories: 1. Characterizing the performance of different clustering algorithms. *J Chem Theory Comput* 2007;3(2312-34.